

# MOLECULAR AND CELLULAR BIOLOGY

## Isolation and biological characterization of mesenchymal stem cells from goose dermis

Jingjing Wang,<sup>\*,†,1</sup> Xulun Wu,<sup>\*,1</sup> Yanjie Zheng,<sup>\*,†</sup> Hebao Wen,<sup>\*,§</sup> Hongda Ji,<sup>\*,†</sup> Yuhua Zhao,<sup>†</sup> and Weijun Guan<sup>\*,2</sup>

<sup>\*</sup>*Institute of Animal Science, Chinese Academy of Agricultural Sciences, Beijing 100193, China;* <sup>†</sup>*School of kinesiology and health, Harbin Institute of Physical Education, Harbin, Heilongjiang province 150008, China;* <sup>‡</sup>*School of Life Sciences, Jiamusi University, Jiamusi, Heilongjiang province 154007, China;* and <sup>§</sup>*School of sports science, Mudanjiang Normal University, Mudanjiang, Heilongjiang province 157011, China*

**ABSTRACT** The skin is a natural target of stem cell research because of its large size and easy accessibility. Cutaneous mesenchymal stem cells have shown to be a promising source of various adult stem cell or progenitor cell populations, which provide an important source of stem cell-based investigation. Nowadays, much work has been done on dermal-derived mesenchymal stem cells (DMSCs) from humans, mice, sheep, and other mammals, but the literature on avian species has been rarely reported. As an animal model, the goose is an endemic species abounding in dermal tissues which is important in the global economy. In this study, we isolated and established the mesenchymal stem cell line from dermis tissue of goose, which were subcultured to passage 21 in vitro without loss of their functional integrity in terms of morphology, renewal capacity, and presence of mesenchymal stem cell markers. Cryopreser-

vation and resuscitation were also observed in different passages. To investigate the biological characteristics of goose DMSCs, immunofluorescence, reverse transcription-polymerase chain reaction, and flow cytometry were used to detect the characteristic surface markers. Growth curves and the capacity of colony forming were performed to test the self-renew and proliferative ability. Furthermore, the DMSCs are induced to osteoblasts, adipocytes, and chondrocytes in vitro. Our results suggest that DMSCs isolated from goose embryos possess similar biological characteristics to those from other species. The methods in establishment and cultivation of goose DMSCs line demonstrated a good self-renew and expansion potential in vitro, which provided a technological platform for preserving the valuable genetic resources of poultry and a great inspiration for in vitro investigation of avian MSCs.

**Key words:** goose, dermis, mesenchymal stem cell (MSC), biological characterization

2018 Poultry Science 97:3236–3247  
<http://dx.doi.org/10.3382/ps/pey178>

### INTRODUCTION

Mesenchymal stem cells (MSCs) are well known for their potential therapeutic value on clinical use because of their high proliferative capacity, ability to differentiate into multiple lineages, and ability to migrate into injured organs and cancers (Panes et al., 2016; Mohr and Zwacka, 2018). Since obtaining large numbers of MSCs from bone marrow has proven to be low frequencies, invasive and limited expansion capacity of cells, alternative cell sources that could be more favorable for large-scale applications have been pursued.

Skin is the most easily accessible solid tissue source and has been shown to be a promising source of vari-

ous adult stem cell or progenitor cell populations, such as epidermal stem cells (Kim et al., 2004), follicle stem cells (Xi et al., 2003), and dermal progenitors (Shyer et al., 2017). Skin of birds and mammals are composed of epidermis and dermis. Skin appendages, such as feathers and hair follicles, arise from their organ germs through reciprocal epithelial-mesenchymal interactions during embryonic skin development, which have contributed to the studies of embryonic organogenesis and biological pattern formation (Ishida and Mitsui, 2016). The dermis is a source of progenitor cells and stem cells for multiple lineages (Sellheyer and Krahl, 2010). MSCs isolated from avian dermis can be differentiated into adipocytes, osteoblasts, and neurons (Young et al., 1995; Gao et al., 2013). It has been found that avian feather follicular cells (FFC) had MSC-like characteristics with regard to gene expression, protein expression, and adipocyte differentiation. In addition, these FFC could also be programmed into pluripotent stem cells

© 2018 Poultry Science Association Inc.

Received February 4, 2018.

Accepted May 9, 2018.

<sup>1</sup>These authors contributed equally to this work.

<sup>1</sup>Corresponding author: [weijunguan301@gmail.com](mailto:weijunguan301@gmail.com)

**Table 1.** The primer information for dermal-derived mesenchymal stem cells identification.

Gene name	Sequences (5'→3')	Product length (bp)	T <sub>m</sub> (°C)	Gene ID
CD29	S: CAGCAAGGTGGAAGTGACTG A: TGGCTGGATCTGTGTAATGG	288	60	1,06,042,674
CD44	S: TCCATCAGGAGATCCAGTCC A: GCTGACCTGGTTGTGACG	317	59	1,06,044,445
CD71	S: GCCTGATCTGAAGAGCCTGT A: TAACTGTGCCGGTCTCACTG	302	59	1,06,044,826
CD73	S: GGAGGAAGGTGCCAGTTGTA A: AAGCACAGCATCACAGAGCA	290	60	1,06,035,383
CD90	S: CAGTGCCAGATGATCAAGGA A: ATCTGGTTGCCGGTGTAGTC	299	58	1,06,039,744
CD105	S: CTGGCACCTACAAGATCACG A: GGCTGGAGCATTAAAGAGCAG	298	59	1,06,047,274
CD34	S: ACACAGCCACACGTAGCAAG A: CCTGGAGCACATCTGTAGCA	304	60	1,06,041,258
VIM	S: GGAGCAGCAGAACAAGATCC A: GAGGCATTGTCAACATCCTG	306	60	1,06,030,144
CD45	S: ACTGGCCATCAATGGAGAAC A: ATAGGTTCCAGTGCGTCCAA	296	60	1,06,041,956
BGLAP	S: ATGAGGAGTCTGCTGGCACT A: CTCATGCATCTGCTCCATTG	216	60	1,06,045,799
OPN	S: CCGACGAGTCTGATGAGGTT A: CTCTTGTCAGCCACTCTCC	319	59	1,06,041,870
PPAR- $\gamma$	S: GGAGGCAGTGCAGGAGATTA A: AATATTGCCAGGTCGCTGTC	291	60	1,06,040,065
LPL	S: GCCTGACCAAGAAGAAGGTG A: GGATCGTTCGTGAGAGCATT	305	60	1,06,040,417
COL2A1	S: GAGACTGGAGAGGCTGGAGA A: CTCATCGCCGTAGCTGAAAGT	288	60	1,06,049,583
ACAN	S: GGAGGAGAACGTGACCAGAG A: CGAAGGAGAAGGCGTATCTG	299	59	1,06,036,508
GAPDH	S: CTGGTGCCGAATATGTTGTG A: GGCCATCCACTGTCTTCTGT	303	60	1,06,047,846

S, sense; A, antisense; bp, base pairs.

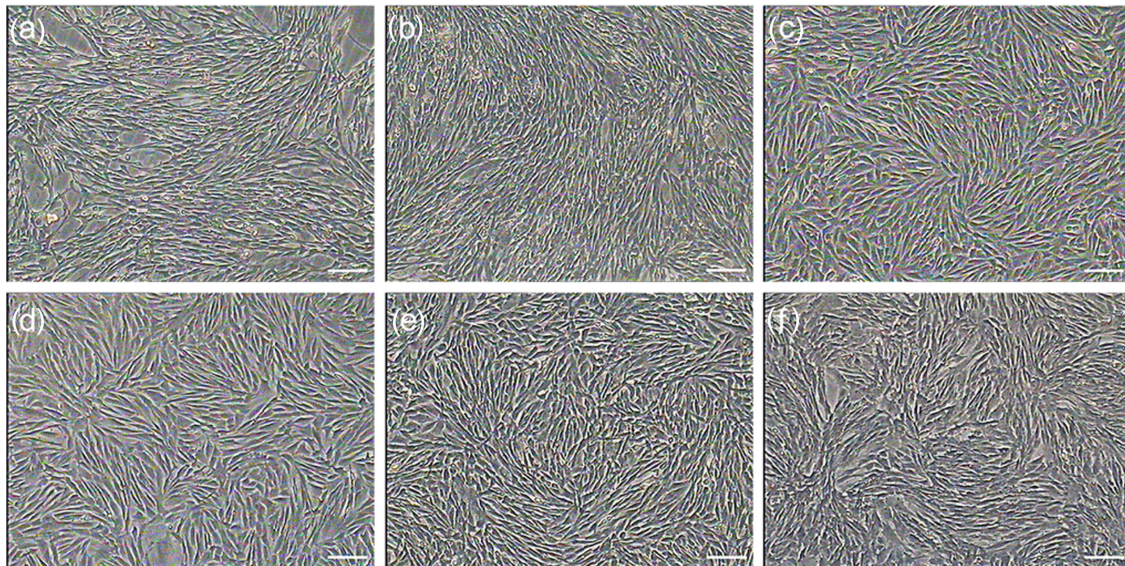


**Figure 1.** Morphology of primary cultured and subcultured dermal-derived mesenchymal stem cells (DMSCs). (a) On day 3 of culture, DMSCs began to elongate, with tiny minority of cells showed irregular shape. (b) Five days after culture, DMSCs exhibited a fibroblast-like morphology and were confluent rapidly. (c) DMSCs at P1. (d) DMSCs at P3. (e) DMSCs at P21. Cells at P3 and P21 were homogeneous with a typical long spindle-shape. (f) DMSCs at P21 with few cells showing signs of senescence (scale bar = 100  $\mu$ m).

(iPSC) considered as representative tools for conservation of animal genetic resources (Kim et al., 2017). Previous studies have shown that the transplanted dermal-derived mesenchymal cells (DMCs) promoted survival and wound healing (Shi et al., 2004). Recently, DMCs have shown promising therapeutic effect on liver injury (Tan et al., 2016) and characteristics for cartilage

tissue engineering (Kalpakci et al., 2014). In addition, DMCs can also decrease the incidence and severity of acute GVHD during MHC-mismatched stem cell transplantation in mice (Gao et al., 2014).

Current research of stem cells focuses on humans, mice, rabbits, and other mammals, but little research has been performed on geese. As an animal model,

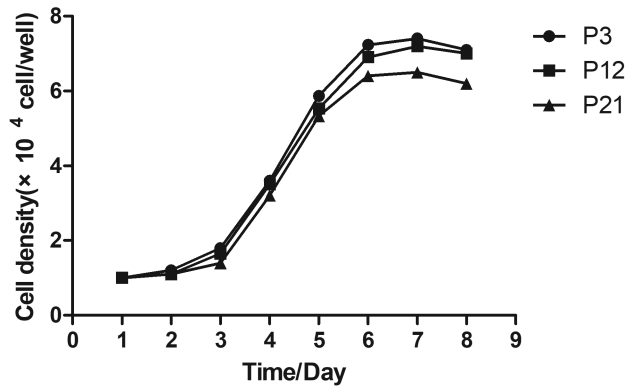


**Figure 2.** Growth curves of dermal-derived mesenchymal stem cells at P3, P12, and P21. Growth curves had a typical sigmoidal shape, indicating the latent, exponential growth, and stationary phases.

the goose possesses abundant dermal tissues, which may contain ample source of MSCs and easy to acquire MSCs for cell-based investigation. Furthermore, the goose is an endemic species that is important in the global economy. In this study, we carried out a pilot study on the separation, culture, and differentiation potential of MSCs from goose embryo dermis, and hence provided great inspiration for in vitro investigation of avian MSCs as well as a new method to conserve the valuable genetic resources of avian species.

## MATERIALS AND METHODS

Animals used for this study and all procedures were in accordance with ethical standards of the Institutional Animal Care and Use Committee at Chinese Academy of Agriculture sciences. The welfare of the animals was ensured during the sampling process.

### Isolation and Culture of Dermal-Derived Mesenchymal Stem Cells

Dorsal skin tissues were isolated from 26-d-old gosling embryos and rinsed over 5 times in PBS. The dermal layer was isolated from the epidermal layer by digestion with 0.25% dispase II (Gibco, USA) for 1.5 to 2 h at 37°C. The dermis was cut into approximately 1 cm<sup>2</sup> pieces and then digested with 0.25% trypsin (Gibco) for about 20 min. Then, the enzymatic activity was neutralized with equal DMEM (**Dulbecco's modified Eagle's medium**) containing 10% fetal bovine serum (**FBS**) (Gibco). The resulting suspension was filtered through a 74- $\mu$ m mesh sieve and then centrifuged at 1200 rpm for 8 min at room temperature. After the supernatant was discarded, the pellet was resuspended in complete medium containing DMEM/F-12 Ham's (Gibco), 10% FBS (Biochrom), 10 ng/mL human basic fibroblast growth factor (PeproTech, USA),

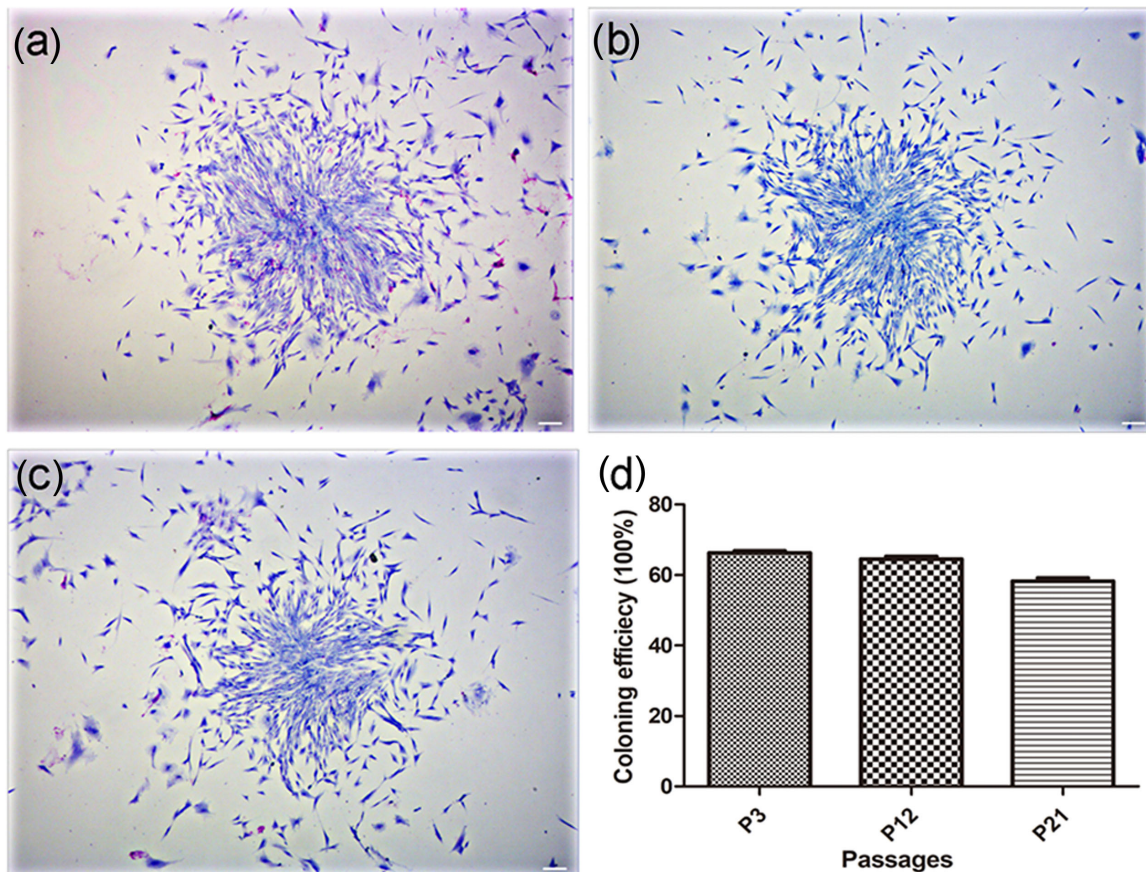


**Figure 3.** Colony-forming efficiency of goose dermal-derived mesenchymal stem cells (DMSCs). Colonies with the morphology of DMSCs were cultured for 1 wk. (a) P3. (b) P12. (c) P21 (scale bar = 100  $\mu$ m). (d) Bar chart showing the cloning rates for different passages of DMSCs.

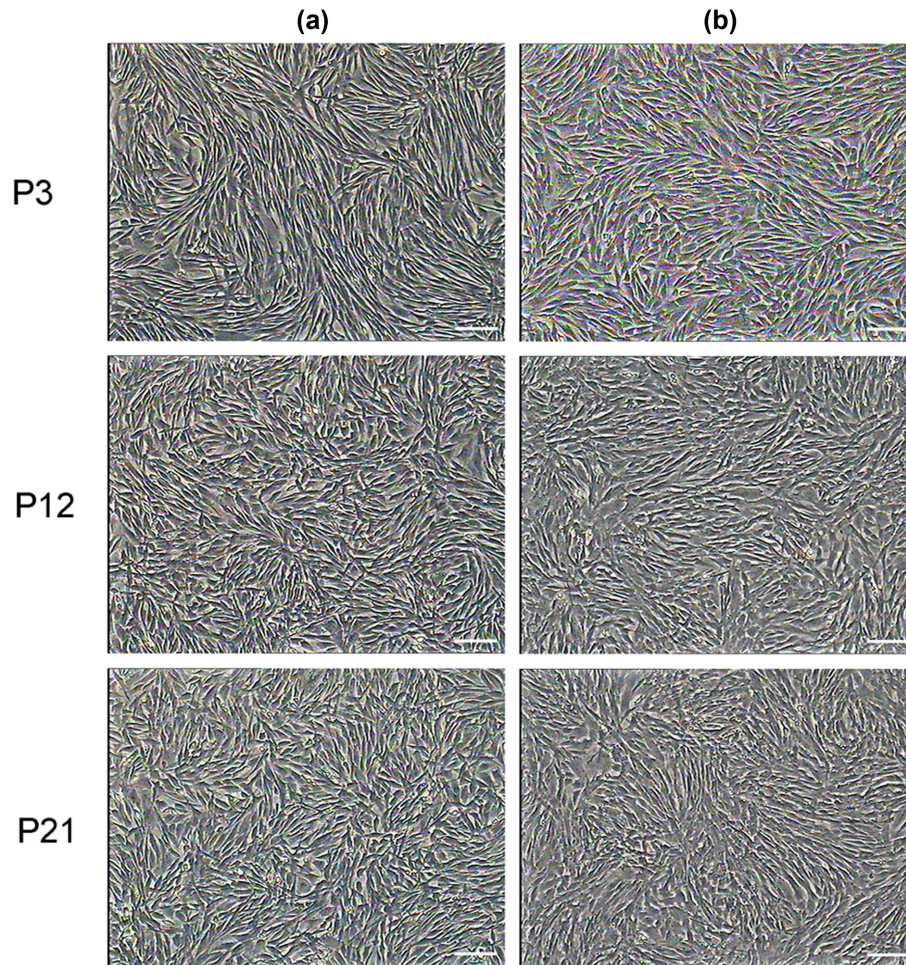


**Figure 4.** Dermal-derived mesenchymal stem cells before freezing (A) and after recovery (B) at 3 passages. There was no significant varies among different passages (scale bar = 100  $\mu$ m).

**Table 2.** Cell survival rate before freezing and after recovery at different passages.

Passages	P3	P12	P21
Before freezing	98.5% $\pm$ 0.4%	97.4% $\pm$ 0.2%	96.6% $\pm$ 0.3%
After recovery	94.2% $\pm$ 0.2%	94.7% $\pm$ 0.5%	93.4% $\pm$ 0.4%

20 ng/mL human epidermal growth factor (PeproTech, USA), 10 ng/ml human LIF (PeproTech, USA), 2 mM L-glutamine, and  $10^4$  IU/mL penicillin/streptomycin. The cells were inoculated in a 60-mm dish and incubated at 37°C with 5% CO<sub>2</sub>. Non-adherent cells were removed 48 h after initial plating by washed with PBS. When cultures reached 90% confluence, cells were trypsinized (0.125% trypsin and 0.02% EDTA) and passaged at a ratio of 1: 2.

### Growth Dynamics

Cells from passages 3, 12, and 21 were used to analyze growth kinetics of dermal-derived mesenchymal stem cells (DMSCs). The cells were harvested and seeded in triplicate in 24-well plates at a density of  $1 \times 10^4$  cells/well. Cell counting was performed on 3 wells each

day for 8 d. Growth curves were plotted according to the mean values, and the population doubling time calculated based on the formula  $PDT = (t - t_0) \log_2 / (\log N_t - \log N_0)$ , where  $t_0$  = starting time of the culture;  $t$  = the termination time of the culture;  $N_0$  = the initial cell number of the culture; and  $N_t$  = the ultimate cell number of the culture (Bai et al., 2013b).

### Colony-Forming Cell Assay

Cells of passage 3, 12, and 21 were seeded in 60 mm dish at a density of  $90 \pm 10$  cells/well cultured for 8 d, and numbers of colony-forming units were counted to calculate colony-forming rate, which is formulated as (colony-forming unit numbers/starting cell number)  $\times$  100%.

### Cryogenic Preservation and Resuscitation

Cells were harvested when reaching about 90% convergence by routine enzyme digestion method. The harvested cell pellet was resuspended in a freezing medium containing 10% dimethylsulfoxide, 50% FBS, and 40% DMEM/F-12. Then, the cells were transferred to liquid

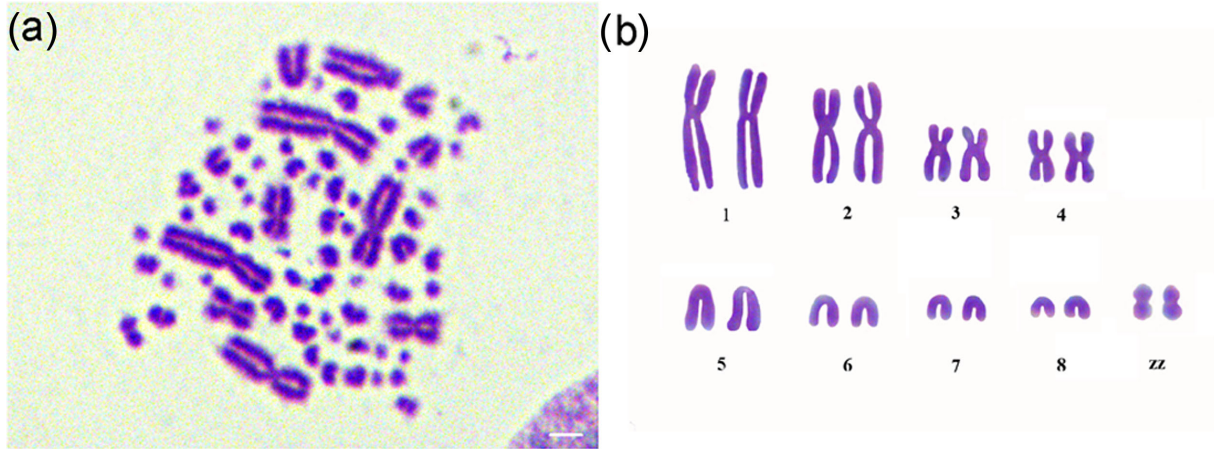


**Figure 5.** Chromosomes at metaphase (a) and karyotype of goose dermal-derived mesenchymal stem cells (b). The number of chromosomes was  $2n = 78$ , including 9 pairs of macrochromosomes, 30 pairs of microchromosomes, and a pair of sex chromosome, type ZZ (scale bar =  $100 \mu\text{m}$ )

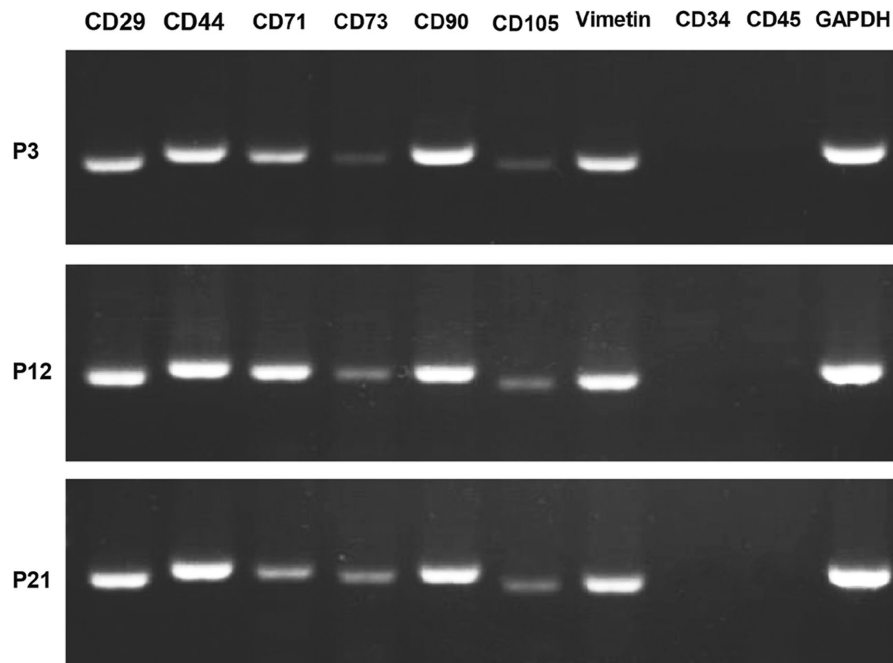


**Figure 6.** Detection of goose dermal-derived mesenchymal stem cells (DMSCs) by RT-PCR. The result showed that DMSCs at different passages expressed *CD29*, *CD44*, *CD90*, *CD71*, *CD73*, *CD105*, and *VIMENTIN*, but negative for *CD34* and *CD45*. *GAPDH* served as the internal control.

nitrogen for long-term storage. When recovered, cells were transferred fast from liquid nitrogen into  $42^{\circ}\text{C}$  water bath, with shaken until thawing. All process should be finished within 1 min. Then, the thawed cells were transferred into the 15 mL centrifuge tube under aseptic conditions. After centrifugation for 8 min at 1200 rpm, the cells were collected and inoculated after the complete medium was added.

### Karyotype Analysis

Karyotype of P10 cells was analyzed as previously described (Baran and Ware, 2007). In brief, cells were harvested when 80 to 90% confluent, subjected to hypotonic treatment and fixed, and the chromosome num-

bers were counted from 100 spreads under an oil immersion objective upon Giemsa staining.

### Gene Expression Analysis of Cell Surface Markers

Dermal-derived mesenchymal stem cells at different passages were collected and total RNA extracted using Trizol reagent (Invitrogen, USA). Total RNA was subjected to reverse transcription, followed by 35 PCR cycles using a 5X All-In-One RT MasterMix kit (abm, Canada). Gene-specific primer pairs are listed in Table 1. Cycling conditions consisted of an initial denaturation step at  $95^{\circ}\text{C}$  for 4 min, then 35 cycles at  $95^{\circ}\text{C}$  for 30 s, 50 to  $60^{\circ}\text{C}$  for 30 s, and  $72^{\circ}\text{C}$  for 2 min.

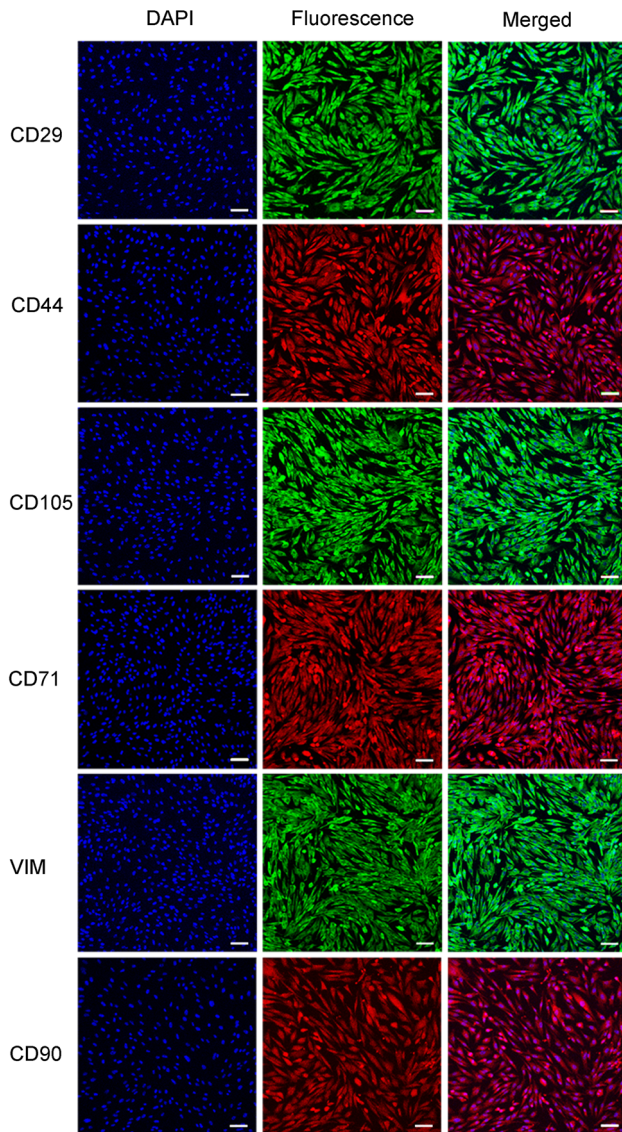


**Figure 7.** Characterization of goose dermal-derived mesenchymal stem cells surface markers by immunofluorescence. The result showed CD29, CD44, CD71, CD90, CD105, and Vimentin were all positive (scale bar = 50  $\mu\text{m}$ ).

PCR products were visualized by electrophoresis on 2.0% (w/v) agarose gels.

### Immunofluorescence

Monolayer cultures of DMSCs were fixed in 4% paraformaldehyde for 20 min and then washed 3 times in PBS. Cells were permeabilized with 0.25% Triton X-100 for 15 min and also washed 3 times in PBS. After blocked with 10% normal goat serum (Bioss, China) at room temperature for 30 min, the cells were incubated in PBS containing the following polyclonal antibodies, respectively: mouse anti-CD29 (1:100; BD, USA), mouse anti-CD44 (1:200; Abcam, USA), rabbit anti-CD90 (1:100; Bioss), rabbit anti-CD71 (1:100, Bioss) and rabbit anti-CD105 (1:200, Bioss) overnight at 4°C. Next day, the primary antibody was removed and cells were washed 3 times with PBS. We then added

FITC-conjugated (1:200, Zhongshan Golden Bridge) or PE-conjugated secondary antibodies (1:200, Bioss) and incubated samples at room temperature in the dark for 1 h. Nuclei were stained with 1  $\mu\text{L}/\text{mL}$  DAPI for 15 min, and then washed 3 times with PBS. Images were acquired using a laser-scanning confocal microscope (Nikon TE-2000-E). As technical controls, PBS was used in place of primary antibodies. Ten randomly selected non-overlapping fields of view were observed and photographed.

### Flow Cytometry

Dermal-derived mesenchymal stem cells were grown until 90% confluent, trypsinized, and pelleted by centrifugation at 1500 rpm for 8 min. Approximately  $3.0 \times 10^6$  cells were resuspended in 1 ml PBS. For flow cytometry analysis, each sample was incubated for 1 h at room temperature with FITC-conjugated antibodies against the following surface markers: CD29, CD44, CD90, CD105, and Vimentin (VIM) (1:200; Bioss). Unstained samples were used to set up a threshold, and the isotype-specific conjugated anti-IgG (1:200, Bioss) was used as a negative control. Finally, each sample was washed in PBS twice and subjected to single channel fluorescently activated cell sorting analysis (Beckman Coulter, Cytomics FC500 MCL).

### Cell Differentiation Assays

Dermal-derived mesenchymal stem cells at P4 were induced to differentiate into osteoblasts by culturing in DMEM/F-12 (Gibco) supplemented with 10% FBS (Biochrom), 1  $\mu\text{M}$  dexamethasone (Sigma), 10 mM  $\beta$ -glycerophosphate (Sigma), and 50 mg/L L-ascorbic-acid-2-phosphate (Sigma) for 12 d. The differentiation potential for osteogenesis was assessed by the mineralization of calcium accumulation by alizarin red S (Leagene) staining and osteocytes specific genes were detected by reverse transcription-polymerase chain reaction (RT-PCR) (Bai et al., 2013a).

For adipogenic differentiation, cells were exposed to L-DMEM supplemented with 10% FBS (Biochrom), 0.1  $\mu\text{M}$  dexamethasone, 0.5 mM (3-Isobutyl-1-methylxanthine, IBMX), 10 mg/L insulin, and 0.2 mM indomethacin (Sigma) for 10 d, with the induction medium changed every 2 d. To assess adipogenic differentiation, intracellular lipid droplets could be observed under the microscope and confirmed by Oil Red O (Leagene) staining and adipocytes specific genes were detected by RT-PCR (Li et al., 2015).

Cells for chondrogenic differentiation were transferred to chondrogenic medium that included DMEM/F12 (Gibco) supplemented with 5% FBS, 1% ITS-G (Gibco), 40 mg/L L-proline (Sigma), 0.1  $\mu\text{M}$  dexamethasone, 50 mg/L L-ascorbic acid, and 10 ng/mL TGF- $\beta$ 1 (PeproTech). Cells were incubated at 37°C and 5%  $\text{CO}_2$  and media changed every

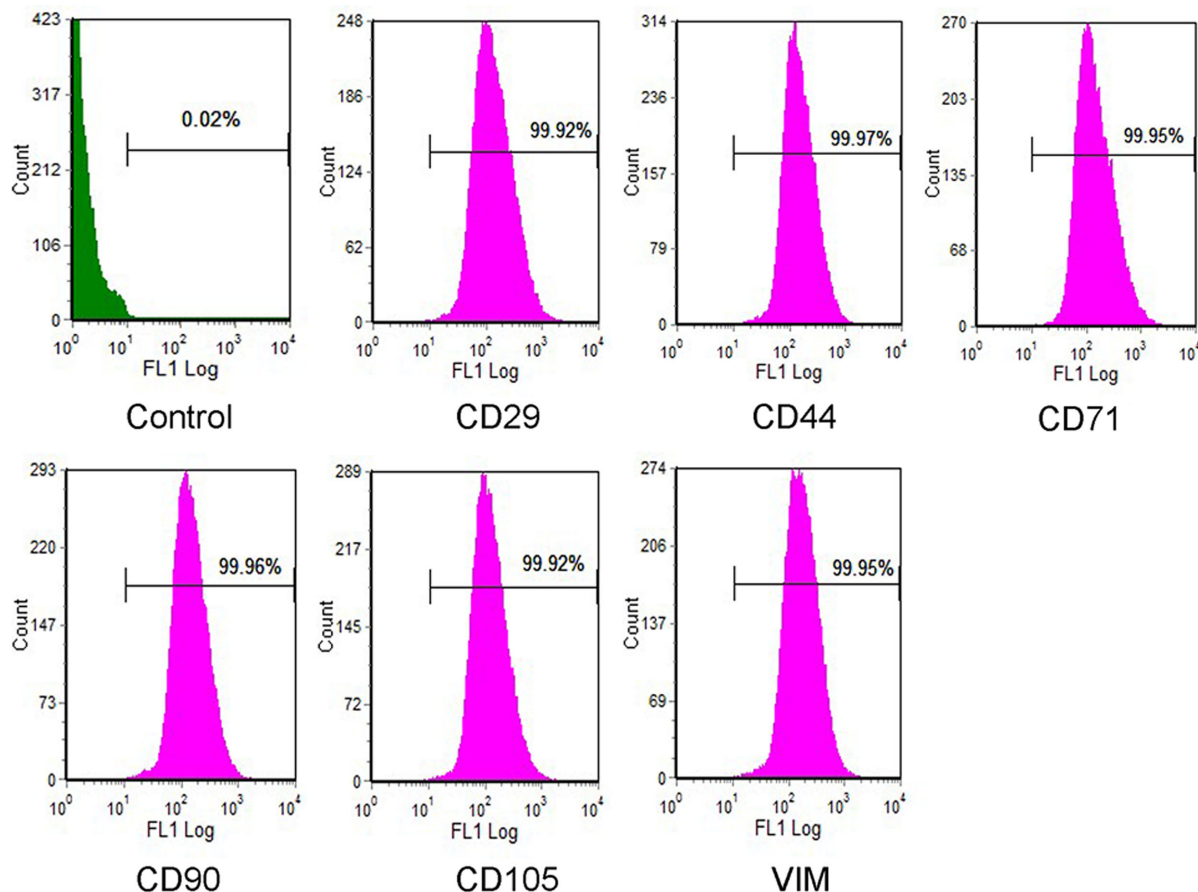


**Figure 8.** Flow cytometric analysis of goose dermal-derived mesenchymal stem cells (DMSCs). Cells were labeled for CD29 (99.92%), CD44 (99.97%), CD71 (99.95%), CD90 (99.96%), CD105 (99.92%), and Vimentin (99.95%), while control group showed a low positive rate (0.02%), which also demonstrated high purity of DMSCs.

3 d. After 2 wk, the cells were identified by staining with alcian blue (Leagene) and chondrocyte-specific genes were detected further using RT-PCR, compared with those induced before (Ranera et al., 2011). Gene-specific primer pairs are listed in Table 1.

## RESULTS

### Morphological Observation of DMSCs

Primary cells isolated from the dermis adhered to the culture plates after 24 h. About 48 h later, the cells began to elongate, with a small number of polygonous cells, and tiny minority of cells showed irregular shape. After about 5 d, the cells exhibited a fibroblast-like morphology and reached 80 to 90% confluent. Then, the cells were subcultured by using 0.125% trypsin with 0.02% EDTA. The passage cells grew rapidly, and the gradually increased spindle-shaped cells exhibited an apparent swirling-like pattern. After 3 to 4 passages, cell morphology was consistent gradually. There were no obvious morphological differences among different passages and cellular morphology remained stable after serial passages. The DMSCs were cultured up to passage 21 with few cells showing signs of senescence, and still have a strong proliferative potential (Figure 1).

### Growth Kinetics

Growth and proliferation of DMSCs were similar at passage 3 (P3), P12, and P21 shown by the determined growth curves (Figure 2). About 24 h after seeding, there was a lag time or latency phase. Then, the cells proliferated rapidly and entered exponential phase post about 72 h. Along with the cell density increase, proliferation was restrained as a result of contact inhibition and the cells entered the plateau phase at approximately 7 to 8 d and began to degenerate. The PDT was approximately 50.21, 51.46, and 55.03 h for passage 3, passage 12, and passage 21, respectively.

### Colony-Forming Cell Assay

Colony formation was observed under the microscope after 7 d. Through Giemsa staining, the morphology of cell colonies of different passages was shown in Figure 3a. The colony-forming rates were  $66.32\% \pm 0.51\%$ ,  $64.59\% \pm 0.72\%$ , and  $58.27\% \pm 0.88\%$  for P3, P12, and P21, respectively (Figure 3). These results demonstrated the self-renewal capacity of the cultured goose DMSCs, which showed no obvious colony-forming efficiency variations between these 3 passages.

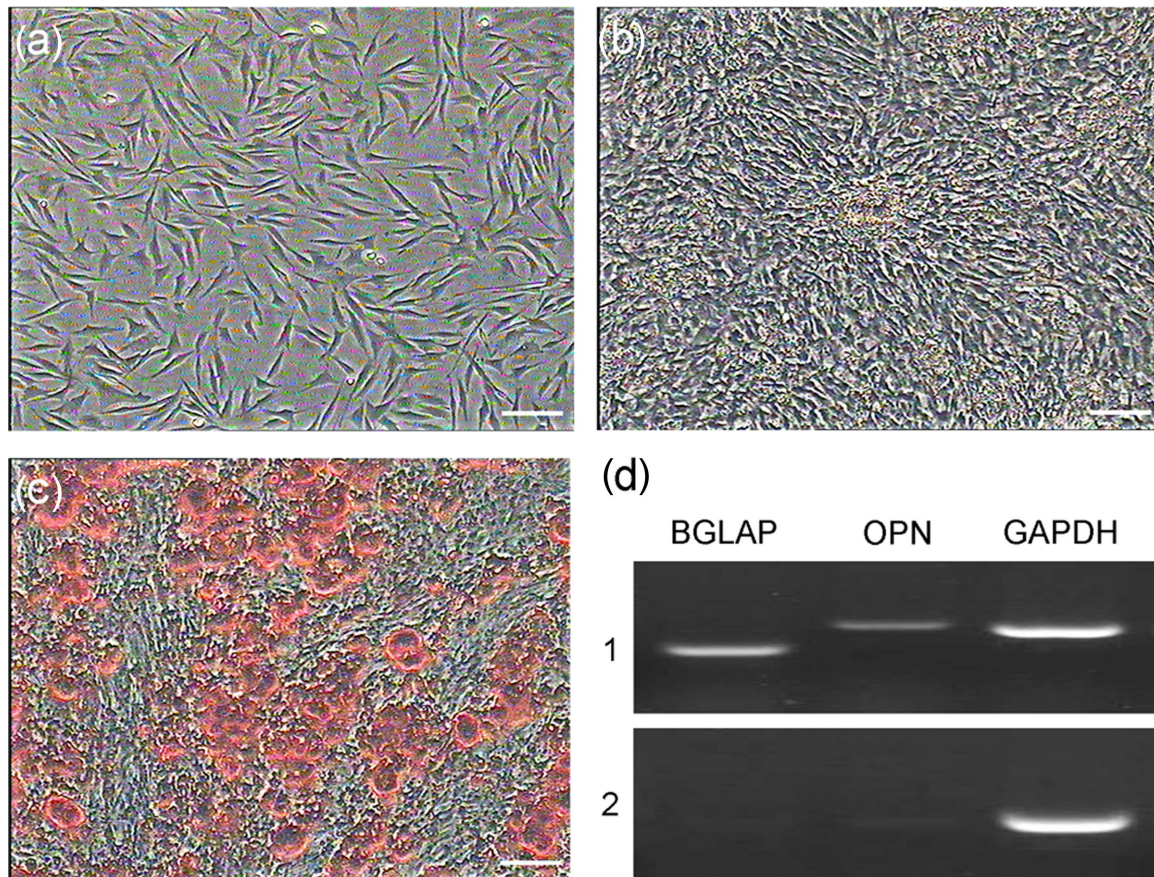


**Figure 9.** Osteogenic differentiation of goose dermal-derived mesenchymal stem cells. (a) Control group. (b) After induction cell morphology altered from fusiform to a larger, round shape with more apparent nodules. (c) Alizarin Red S staining at day 14 post-induction. (d) RT-PCR assays revealed expression of osteoblast-specific genes, including *BGLAP*, *OPN* at day 14 post-induction (1). These genes were not expressed in the control group (2) (scale bar = 100  $\mu\text{m}$ ).

### Cryogenic Resuscitation Rate Analysis

After recovery, the growth state and morphology of cells were normal; there was no significant difference before freezing and after recovery among different passages (Figure 4). The cell survival rate was detected before freezing and after recovery, which were shown in Table 2. Therefore, the freezing storage conditions were appropriate and the DMSCs could be effectively preserved by this way.

### Karyotype Analysis

The diploid chromosome number of goose DMSCs was  $2n = 78$ , consisting of 9 pairs of macrochromosomes and 30 pairs of microchromosomes, with the sex chromosome type was ZZ ( $\sigma^7$ ) (Figure 5).

### Surface Markers of Goose DMSCs

Cells from passages 3, 12, and 21 exhibited no variation in the expression of the following markers: CD29, CD44, CD73, CD71, CD90, CD105, VIM, CD34, and CD45. RT-PCR showed that all markers

were expressed, with the exception of *CD34* and *CD45* (Figure 6). The results of immunofluorescence showed that these cells are positive for CD29, CD44, CD71, CD90, CD105, and VIM (Figure 7). Furthermore, the flow cytometry analysis detected that CD29, CD44, CD71, CD90, CD105, and VIM expressions were all over 99% of the DMSC population, while the control group was observed in a distinct population of 0.02%, which demonstrated high purity of DMSCs (Figure 8).

### Osteogenic Differentiation of Goose DMSCs

After incubation in osteogenic medium for 7 d, DMSCs showed obvious morphological changes. After 14 d of differentiation, the cells became aggregated and formed mineralized nodules that were stained with alizarin red S (Figure 9c). In addition, the number and size of nodules were increased (Figure 9b), whereas control cells showed no perceptible changes (Figure 9a). Osteogenic-specific gene bone gamma-carboxyglutamate protein (*BGLAP*) and osteopontin (*OPN*) were detected by RT-PCR in the induced group but not in the control group (Figure 9d).

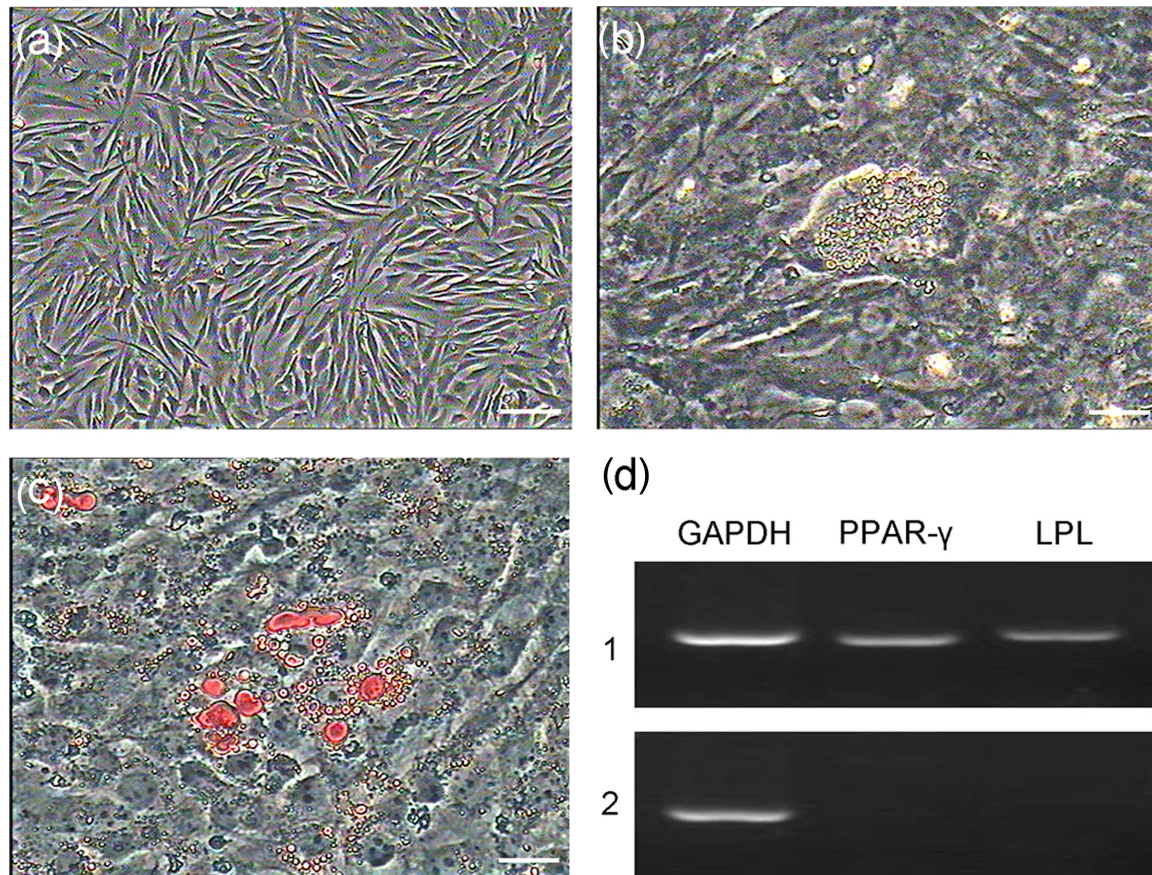


**Figure 10.** Adipogenic differentiation of goose dermal-derived mesenchymal stem cells. (a) Control group (scale bar = 100  $\mu\text{m}$ ). (b) After 14 d of induction, dermal-derived mesenchymal stem cells were changed into oblate with many intracellular lipid droplets (scale bar = 500  $\mu\text{m}$ ). (c) Oil-red O staining for lipid droplets (scale bar = 500  $\mu\text{m}$ ). (d) Expression of adipocyte-specific genes, containing proliferator-activated receptor- $\gamma$  and lipoprotein lipase, was detected by RT-PCR at day 14 post-induction (1). These genes were not expressed in the control group (2).

### Adipogenic Differentiation of Goose DMSCs

In adipogenic medium, cells growth slowed down apparently. Most of the cells changed from a shuttle shape to an oblate shape and contained many intracellular lipid droplets after 7 d. As differentiation progressed, the number of lipid droplets increased and aggregated to form larger droplets (Figure 10b). As a negative control, cells cultured in complete medium were negative for oil red O staining after 14 d (Figure 10a), which differed from the induction group (Figure 10c). After induction, RT-PCR results showed that the cells expressed adipocyte-specific genes peroxisome proliferator-activated receptor- $\gamma$  and lipoprotein lipase, whereas these genes were not expressed in the control group (Figure 10d).

### Chondrogenic Differentiation of Goose DMSCs

Chondrogenic differentiation of goose DMSCs was identified by marked deposition of glycosaminoglycans in the matrix, which was observable after 21 d with Alcian blue staining (Figure 11c). During the time of induction, cells showed obvious morphological changes,

formed small colonies, and proliferated in a relatively low speed. The nuclear to cytoplasm ratio got higher (Figure 11b), while the non-induction group cultured in complete medium showed no such effects (Figure 11a). The presence of chondrocyte-specific gene collagen type II alpha 1 chain and aggrecan confirmed chondrogenic induction for these cell populations (Figure 11d).

## DISCUSSION

Because of the easy accessibility and multidifferentiation, dermal stem cells have been widely used in a variety of fields, including wound healing (Kyung et al., 2007), tissue engineering (Ishida and Mitsui, 2016), and cell reprogramming (Kim et al., 2017). Despite many animal models have been used in research, the characterization of goose MSCs is still limited. In this study, DMSCs have successfully been isolated from the dorsal dermis of 26-d-old goose embryos using the way of trypsin digestion. All the results showed that the biological characteristics of the newly isolated stem cells were stable, and had a good self-renewal and proliferative ability.

Growth curve is a conventional method to detect cell growth rhythm, the result of test showed that the

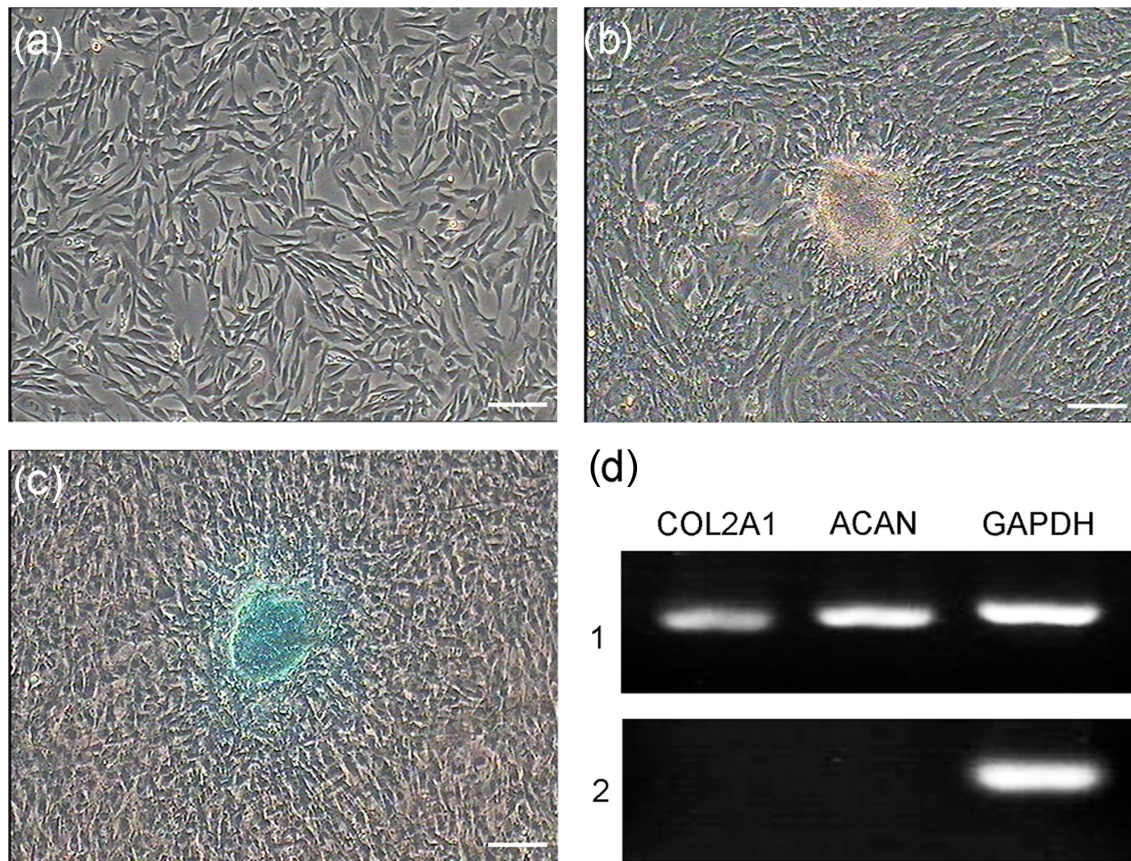


**Figure 11.** Chondrogenic differentiation of goose dermal-derived mesenchymal stem cells. (a) Control group without inducing factors. (b) The cellular configuration expanded with the deposition of glycosaminoglycans in the matrix after induction. (c) Alcian blue staining was observed at day 21 after induction. (d) Chondrocyte-specific genes including collagen type II alpha 1 chain and aggrecan were expressed post-induction (1). While the control group were negative (2) (scale bar = 100  $\mu$ m).

growth curve had a typical “S” shape and had a normal population doubling time. The colony-forming ability is essential for the self-renewal and specific differentiation characteristics of stem cells, which can reflect 2 important traits of the cell, namely population-dependent and proliferative capacity. In this study, colony units of goose DMSCs formed after 7 d showing a good self-renewal and proliferative ability. Karyotype analysis is a major method for distinguishing normal cells from variants. Birds are one of the least examined animal groups due to karyotype specificity, i.e., small chromosomes, a large diploid chromosome number or the division of the chromosomes into macro- and microchromosomes (Wojcik and Smalec, 2011). The DMSCs cultured in this study were all normal diploids and the genetic property of the cells was stable during the passaging sequentially.

Phenotypically, MSC-like dermal stem cells expressed the markers CD29, CD44, CD105, CD71, CD73, and CD90 (Lorenz et al., 2008). In addition, VIM, a mesenchymal marker, was also generally found in MSC-like dermal stem cells (Chen et al., 2007; Huang et al., 2010). So far, the specific markers of DMSCs were not found. In our study, we found that all of these markers above were expressed, which supported the previous data. Moreover, the hematopoietic cell surface antigens such as CD34 and CD45 were negative in the detec-

tion of goose DMSCs, which demonstrated they did not contain dermal hematopoietic cells. CD29, also called  $\beta$ -Integrin, plays a fundamental role in cell adhesion and migration, linking the extracellular matrix to the actin cytoskeleton. Liu’s research demonstrated that integrin  $\beta$ 1 expression by fibroblasts is required for dermal homeostasis; 8 wk after deletion of integrin  $\beta$ 1, the skin is noticeably thinner than that of wild-type mice (Liu and Leask, 2013). CD44 acts as a pivotal role in modulating several diverse behaviors important for adhesion, proliferation, apoptosis, migration, and invasion during development, growth, repair, maintenance, and regression of a wide variety of mesenchymal tissues (Tsuneki and Madri, 2016). CD71 maintaining cellular iron homeostasis is mainly expressed on cycling cells, means on proliferative active cells (Tani et al., 2000). CD73 is a membrane-anchored protein that hydrolyzes extracellular adenosine 5'-monophosphate (AMP) to adenosine in diverse tissues, such as dermis. It has been demonstrated that CD73 could promote anti-inflammatory effects of adenosine in the immune system (Bonner et al., 2012) and attenuate acute injury and inflammation (Volmer et al., 2006), as well as regulate extracellular adenosine involving in dermal fibrogenesis (Fernandez et al., 2013). CD90 has broad non-immunological functions, including apoptotic signaling, leukocyte and melanoma cell

adhesion and migration, tumor suppression and fibroblast proliferation and migration (Rege and Hagood, 2006). Lee's study suggested that CD90 regulated skin wound healing by modulating fibroblast recruitment (Lee et al., 2013). Blocking CD90 RNA at the wound area resulted in an increased expression of TGF- $\beta$ 1 and accelerated the rate at which fibroblasts accumulated during the healing process; decreasing CD90 levels may result in an enlarged wound area and abnormal re-epithelialization, thus delaying the wound healing process.

Multilineage differentiation potentiality has been considered an important quality of MSCs. In vitro, under the action of some inducing factors, DMSCs can differentiate into adipogenic, osteogenic, and other lineages (Bartsch et al., 2005; Lavoie et al., 2009). TGF- $\beta$ 1 is a multifunctional protein that induces gene expression of cartilage-specific molecules, and can facilitate chondrogenic precursor cells differentiating into chondrocytes (Li et al., 2017). Insulin and IBMX are necessary for adipocyte differentiation (Chon and Pappas, 2015). However, the mechanisms of these factors in differentiation need further investigation. In our study, we differentiated goose DMSCs into osteoblasts, adipocytes, and chondrocyte, and relevant genes of these cell types were expressed. In addition, Gao et al. (2013) demonstrated that chicken dermis-derived MSCs could be induced to osteoblasts and adipocytes; however, Kim et al. (2017) found chicken FFC did not differentiate into chondrocytes and osteoblasts, which indicated that different induction factors may affect the differentiation of DMSCs.

## CONCLUSION

In this study, we isolated DMSCs from the dermis of 26-d-old goose embryos and then examined their ability to expand and differentiate in vitro. Cell morphology, surface markers, and biological characteristics were also observed and detected. These results not only provided a technological platform for the establishment of a goose DMSCs line, but also proposed a method to preserve the valuable genetic resources of avian species.

**Conflict of interest.** None declared.

## ACKNOWLEDGMENTS

This research was supported by the National Natural Science Foundation of China (31672404), the Agricultural Science and Technology Innovation Program (ASTIP) (cxgc-ias-01), and the project National Infrastructure of Animal Germplasm Resources (2016 year).

## REFERENCES

Bai, C., L. Hou, Y. Ma, L. Chen, M. Zhang, and W. Guan. 2013a. Isolation and characterization of mesenchymal stem cells from chicken bone marrow. *Cell Tissue Bank* 14:437–451.

- Bai, C., X. Li, L. Hou, M. Zhang, W. Guan, and Y. Ma. 2013b. Biological characterization of chicken mesenchymal stem/progenitor cells from umbilical cord Wharton's jelly. *Mol. Cell. Biochem.* 376:95–102.
- Baran, S. W., and C. B. Ware. 2007. Cryopreservation of rhesus macaque embryonic stem cells. *Stem Cells Dev.* 16:339–344.
- Bartsch, G., J. J. Yoo, P. De Coppi, M. M. Siddiqui, G. Schuch, H. G. Pohl, J. Fuhr, L. Perin, S. Soker, and A. Atala. 2005. Propagation, expansion, and multilineage differentiation of human somatic stem cells from dermal progenitors. *Stem Cells Dev.* 14:337–348.
- Bonner, F., N. Borg, S. Burghoff, and J. Schrader. 2012. Resident cardiac immune cells and expression of the ectonucleotidase enzymes CD39 and CD73 after ischemic injury. *PLoS One* 7: e34730.
- Chen, F. G., W. J. Zhang, D. Bi, W. Liu, X. Wei, F. F. Chen, L. Zhu, L. Cui, and Y. Cao. 2007. Clonal analysis of nestin vimentin+ multipotent fibroblasts isolated from human dermis. *J. Cell Sci.* 120:2875–2883.
- Chon, S. H., and A. Pappas. 2015. Differentiation and characterization of human facial subcutaneous adipocytes. *Adipocyte* 4: 13–21.
- Fernandez, P., M. Perez-Aso, G. Smith, T. Wilder, S. Trzaska, L. Chiriboga, A. Franks, Jr., S. C. Robson, B. N. Cronstein, and E. S. L. Chan. 2013. Extracellular generation of adenosine by the ectonucleotidases CD39 and CD73 promotes dermal fibrosis. *Am. J. Pathol.* 183:1740–1746.
- Gao, L., F. Liu, L. Tan, T. Liu, Z. Chen, and C. Shi. 2014. The immunosuppressive properties of non-cultured dermal-derived mesenchymal stromal cells and the control of graft-versus-host disease. *Biomaterials* 35:3582–3588.
- Gao, Y., C. Bai, H. Xiong, Q. Li, Z. Shan, L. Huang, Y. Ma, and W. Guan. 2013. Isolation and characterization of chicken dermis-derived mesenchymal stem/progenitor cells. *BioMed Res. Int.* 2013:1–8.
- Huang, H. I., S. K. Chen, Q. D. Ling, C. C. Chien, H. T. Liu, and S. H. Chan. 2010. Multilineage differentiation potential of fibroblast-like stromal cells derived from human skin. *Tissue Eng. Part A* 16:1491–1501.
- Ishida, K., and T. Mitsui. 2016. Generation of bioengineered feather buds on a reconstructed chick skin from dissociated epithelial and mesenchymal cells. *Develop. Growth Differ.* 58:303–314.
- Kalpaki, K. N., W. E. Brown, J. C. Hu, and K. A. Athanasiou. 2014. Cartilage tissue engineering using dermis isolated adult stem cells: the use of hypoxia during expansion versus chondrogenic differentiation. *PLoS One* 9:e98570.
- Kim, D. S., H. J. Cho, H. R. Choi, S. B. Kwon, and K. C. Park. 2004. Isolation of human epidermal stem cells by adherence and the reconstruction of skin equivalents. *Cell. Mol. Life Sci.* 61:2774–2781.
- Kim, Y. M., Y. H. Park, J. M. Lim, H. Jung, and J. Y. Han. 2017. Technical note: Induction of pluripotent stem cell-like cells from chicken feather follicle cells. *J. Anim. Sci.* 95:3479–3486.
- Kyung, K. S., C. W. Ho, and C. B. Kwan. 2007. Potential therapeutic clue of skin-derived progenitor cells following cytokine-mediated signal overexpressed in injured spinal cord. *Tissue Eng.* 13:1247–1258.
- Lavoie, J. F., J. A. Biernaskie, Y. Chen, D. Bagli, B. Alman, D. R. Kaplan, and F. D. Miller. 2009. Skin-derived precursors differentiate into skeletogenic cell types and contribute to bone repair. *Stem Cells Dev.* 18:893–906.
- Lee, M. J., J. O. Shin, and H. S. Jung. 2013. Thy-1 knockdown retards wound repair in mouse skin. *J. Dermatol. Sci.* 69:95–104.
- Li, L., Y. Ma, X. Li, X. Li, C. Bai, M. Ji, S. Zhang, W. Guan, and J. Li. 2015. Isolation, culture, and characterization of chicken cartilage stem/progenitor cells. *BioMed Res. Int.* 2015:586290.
- Li, Y., A. Y. Tian, J. Ophene, M. Y. Tian, Z. Yao, S. Chen, H. Li, X. Sun, and H. Du. 2017. TGF-beta stimulates endochondral differentiation after denervation. *Int. J. Med. Sci.* 14:382–389.
- Liu, S., and A. Leask. 2013. Integrin beta1 is required for dermal homeostasis. *J. Invest. Dermatol.* 133:899–906.

- Lorenz, K., M. Sicker, E. Schmelzer, T. Rupf, J. Salvetter, M. Schulz-Siegmund, and A. Bader. 2008. Multilineage differentiation potential of human dermal skin-derived fibroblasts. *Exp. Dermatol.* 17:925–932.
- Mohr, A., and R. Zwacka. 2018. The future of mesenchymal stem cell-based therapeutic approaches for cancer - From cells to ghosts. *Cancer Lett.* 414:239–249.
- Panes, J., D. Garcia-Olmo, G. Van Assche, J. F. Colombel, W. Reinisch, D. C. Baumgart, A. Dignass, M. Nachury, M. Ferrante, L. Kazemi-Shirazi, J. C. Grimaud, F. de la Portilla, E. Goldin, M. P. Richard, A. Leselbaum, and S. Danese. 2016. Expanded allogeneic adipose-derived mesenchymal stem cells (Cx601) for complex perianal fistulas in Crohn's disease: a phase 3 randomised, double-blind controlled trial. *Lancet North Am. Ed.* 388:1281–1290.
- Ranera, B., J. Lyahyai, A. Romero, F. J. Vazquez, A. R. Remacha, M. L. Bernal, P. Zaragoza, C. Rodellar, and I. Martin-Burriel. 2011. Immunophenotype and gene expression profiles of cell surface markers of mesenchymal stem cells derived from equine bone marrow and adipose tissue. *Vet. Immunol. Immunopathol.* 144:147–154.
- Rege, T. A., and J. S. Hagoood. 2006. Thy-1 as a regulator of cell-cell and cell-matrix interactions in axon regeneration, apoptosis, adhesion, migration, cancer, and fibrosis. *FASEB J.* 20:1045–1054.
- Sellheyer, K., and D. Krahl. 2010. Skin mesenchymal stem cells: prospects for clinical dermatology. *J. Am. Acad. Dermatol.* 63:859–865.
- Shi, C., T. Cheng, Y. Su, Y. Mai, J. Qu, S. Lou, X. Ran, H. Xu, and C. Luo. 2004. Transplantation of dermal multipotent cells promotes survival and wound healing in rats with combined radiation and wound injury. *Radiat. Res.* 162:56–63.
- Shyer, A. E., A. R. Rodrigues, G. G. Schroeder, E. Kassianidou, S. Kumar, and R. M. Harland. 2017. Emergent cellular self-organization and mechanosensation initiate follicle pattern in the avian skin. *Science* 357:811–815.
- Tan, L., T. Dai, D. Liu, Z. Chen, L. Wu, L. Gao, Y. Wang, and C. Shi. 2016. Contribution of dermal-derived mesenchymal cells during liver repair in two different experimental models. *Sci. Rep.* 6:25314.
- Tani, H., R. J. Morris, and P. Kaur. 2000. Enrichment for murine keratinocyte stem cells based on cell surface phenotype. *Proc. Natl. Acad. Sci.* 97:10960–10965.
- Tsuneki, M., and J. A. Madri. 2016. CD44 influences fibroblast behaviors via modulation of Cell-Cell and Cell-Matrix interactions, affecting survivin and hippo pathways. *J. Cell. Physiol.* 231:731–743.
- Volmer, J. B., L. F. Thompson, and M. R. Blackburn. 2006. Ecto-5'-nucleotidase (CD73)-mediated adenosine production is tissue protective in a model of bleomycin-induced lung injury. *J. Immunol.* 176:4449–4458.
- Wojcik, E., and E. Smalec. 2011. Comparing the karyotype of the European domestic goose and the Asian goose on the basis of the karyotype of their interspecific cross-breed, using the RBG chromosome staining technique. *Folia Biol.* 59:107–113.
- Xi, Y., Y. Nada, T. Soh, N. Fujihara, and M. A. Hattori. 2003. Establishment of feather follicle stem cells as potential vehicles for delivering exogenous genes in birds. *J. Reprod. Dev.* 49:213–219.
- Young, H. E., M. L. Mancini, R. P. Wright, J. C. Smith, A. C. Black, Jr., C. R. Reagan, and P. A. Lucas. 1995. Mesenchymal stem cells reside within the connective tissues of many organs. *Dev. Dyn.* 202:137–144.